Nuclear Instruments and Methods in Physics Research B xxx (2017) xxx–xxx

Contents lists available at ScienceDirect

Nuclear Instruments and Methods in Physics Research B

journal homepage: www.elsevier.com/locate/nimb

Simultaneous use and self-consistent analyses of μ-PIXE and μ-EBS for the characterization of corrosion layers grown on ancient coins

J. Cruz [a,*], V. Corregidor [b], L.C. Alves [c]

[a] LIBPhys-UNL, DF, FCT, Universidade NOVA de Lisboa, 2829-516 Monte da Caparica, Portugal
[b] IPFN, IST-UL, Campus Tecnológico e Nuclear, E.N. 10, 2695-066 Sacavém, Portugal
[c] C2TN, IST-UL, Campus Tecnológico e Nuclear, E.N. 10, 2695-066 Sacavém, Portugal

ARTICLE INFO

Article history:
Received 1 August 2016
Received in revised form 14 December 2016
Accepted 7 February 2017
Available online xxxx

Keywords:
Coins corrosion
IBA techniques
Self-consistent analysis

ABSTRACT

The study of corrosion products in two XVI century coins through the simultaneous and self-consistent μ-PIXE and μ-EBS spectra analyses is presented in this work.

The fitted spectra give consistent results, showing the feasibility of this approach to determine in a fast and non-destructive way the elemental composition and concentration depth profiles of the corrosion layers.

1. Introduction

The study of corrosion products in ancient metal artifacts, namely coins, gives important information about degradation mechanisms that occurred or are still occurring, their extension, and which conservation/restauration procedures can be effective to stabilize the metallic surface. This study is also important for forensic purposes as it can help to identify forged artifacts with a patina artificially grown.

Corroded surface composition and thickness depends on the coin alloy and exposure time to environmental conditions, such as humidity, contact with other metals and type of soil for coins recovered from archaeological sites. Old coins usually show a large number of trace elements (e.g. Fe, Ni, Sb, Mn, Ti, Co and As – some of them are natural impurities of the metal/alloy used) to which it can be added C, O, Al, Si, Ca, K, Cl, Br, P, Na, Fe, etc, from exposure to the environment.

PIXE (Particle Induced X-ray Emission) is an IBA (Ion Beam Analysis) technique widely used in the study of modern and ancient coins [1–4], but since it does not give information about elemental depth distribution and about elements lighter than sodium, it is sometimes combined with EBS (Elastic Backscattering Spectrometry), which gives information about the depth distribution of the elements detected by PIXE, and can also detect light elements such as carbon and oxygen. This combination has been applied to a limited extent in the study of coins [5–7] with the PIXE and EBS spectra being acquired simultaneously but analyzed separately, which required a considerable effort in order to get a self-consistent solution for the different spectra.

In 2006, C. Pascual-Izarra et al. presented the LibCPIXE software module [8] capable of simulating PIXE X-ray yields in layered targets that once integrated into the DataFurnace code [9] allows the simultaneous and self-consistent automatic analysis of several PIXE and EBS spectra. This automation capacity introduced the concept of "Total IBA" that has been used in several analyses although its full potential is still incompletely realized [10 and references therein].

In this work, we apply the "Total IBA" concept, with PIXE and EBS techniques, to study the corrosion layer of two Portuguese coins from the XVI century. To our knowledge, this is the first time this concept is applied to this kind of samples.

2. Materials and methods

2.1. Studied coins

The two coins taken under study belong to the Portuguese second dynasty: one 5 Reais silver-copper coin (91.66 Ag wt.% as stipulated by decree of law, m = 0.50 g; ∅ = 14 mm) minted during D. Manuel I reign (1495–1521) – Fig. 1-left panel; and one 2 Reais copper coin (m = 3.26 g; ∅ = 25 mm) minted during D. António regency (1580–1583) – Fig. 1-right panel.

* Corresponding author.
E-mail address: jdc@fct.unl.pt (J. Cruz).

http://dx.doi.org/10.1016/j.nimb.2017.02.010
0168-583X/

Fig. 1. Photos of studied coins. Left panel: Reverse of the 5 Reais silver-copper coin minted during king Manuel I reign (1495–1521). Right panel: Obverse of the 2 Reais copper coin minted during D. António regency (1580–1583). The squares indicate the areas covered by the 2D PIXE maps (scan 2640 × 2640 μm^2); The dots indicate the locations of PIXE + EBS point analysis (3 × 4 μm^2).

The coins were in reasonable state of preservation, and both presented a corrosion layer of unknown thickness and composition. The storage/preservation conditions are unknown.

2.2. Experimental procedure

The studied coins were cleaned with alcohol in an ultrasonic cleaning bath before the measurements and their surfaces optically inspected with an Olympus SZX9 stereo microscope for area selection to be probed by the ion microbeam and then obtain the local X-ray surface elemental distribution maps. These maps allowed to identify regions with different corrosion patterns.

PIXE and EBS spectra were obtained simultaneously under vacuum conditions (P ≈ 5 × 10^{-6} mbar) at the microprobe beam line of the 2.5 MV Van de Graaff Accelerator of the CTN/IST (Lisbon, Portugal) [11] using a 2.0 MeV proton beam at normal incidence. The beam dimensions, 3 × 4 μm^2, gives the capacity to distinguish surface inhomogeneities down to the micrometer size.

The PIXE spectra were collected using a 8 μm thick Be windowed Si(Li) detector with 145 eV resolution placed at 135° to the beam direction. It was operated with different absorbers: for the 5 Reais coin, a 250 μm thick Mylar foil was used, filtering approximately 98% of the high intensity Ag L lines. This was required in order to keep the dead time below 10% since the acquisition system is composed of a single multiplexed ADC; for the 2 Reais coin, it was used a 50 μm thick Mylar foil (in order to protect the detector from backscattered protons).

The EBS spectra were collected with a 200 mm^2 PIPS detector with 30 keV resolution in Cornell geometry placed at 140° to the beam direction.

Microprobe operation and basic data manipulation, including X-ray surface elemental distribution mapping, was achieved through the OMDAQ software code [12]. Beam scans over the surface of the samples can range up to 2640 × 2640 μm^2. In selected points of interest, PIXE spectra evaluation and quantification was done with the GUPIXWIN [13] code, assuming a bulk sample. The results, which include the elemental concentration and the peak area of each X-ray line, were used as input in the DataFurnace code [9] to fit the EBS spectra, thus providing a self-consistent elemental depth profiles for each selected point of interest. This procedure was implemented assuming local search fitting, and some constraints were imposed depending on the studied coin (see details in next section). The beam straggling was calculated assuming Chu correction with Tschälar effect; the double scattering contribution and the pulse pile-up effect (considering the Molodtsov and Gurbich algorithm [14]) were calculated and the non-Rutherford cross sections for C and O were included in the fitting model [15].

In terms of sensitivity, for PIXE the lowest limit of detection (LOD) can be as low as a few μg/g. The accuracy of the measurements was considered to be only dependent on the counting statistics and fit error. So, in general, major elements concentrations are obtained with accuracy below 2%. For the trace elements, this accuracy degrades, being about 5% for absolute concentrations around 0.1% and about 20% for elements at a lower concentration level (<0.01%). For EBS, the LOD is around 3% and the depth resolution of concentration profiles is estimated to be around 100 nm. For both techniques, the accessible depth is a few micrometers.

3. Results and discussion

3.1. Silver-Copper coin (5 Reais)

A 2640 × 2640 μm^2 surface scan of was taken in the area highlighted by the open square in Fig. 1a. The detected X-rays indicated the presence of Ag and Cu, which are the coin's main constituents, and also Fe, Pb and Br. Fig. 2 shows the X-ray surface elemental

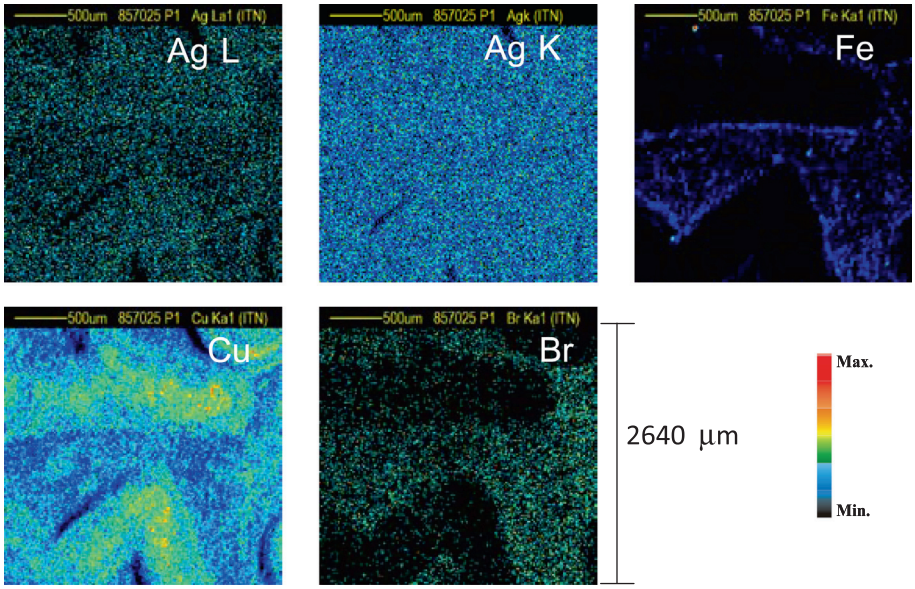

Fig. 2. Silver-copper coin PIXE elemental surface maps for Ag L$_\alpha$, Ag K$_\alpha$, Fe K$_\alpha$, Cu K$_\alpha$ and Br K$_\alpha$ obtained with a 2 MeV proton beam (scan 2640 × 2640 μm^2).

Please cite this article in press as: J. Cruz et al., Simultaneous use and self-consistent analyses of μ-PIXE and μ-EBS for the characterization of corrosion layers grown on ancient coins, Nucl. Instr. Meth. B (2017), http://dx.doi.org/10.1016/j.nimb.2017.02.010

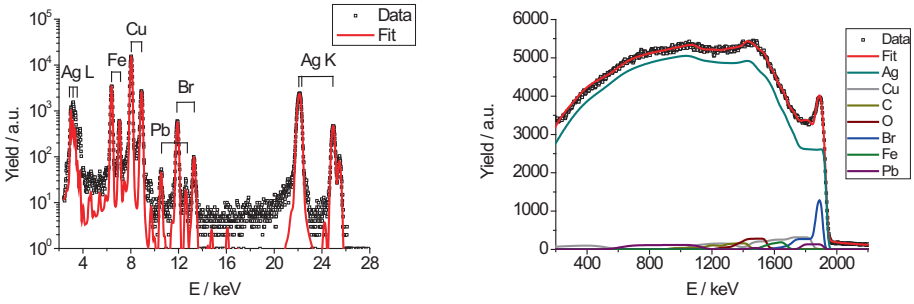

Fig. 3. μ-PIXE and μ-EBS spectra taken simultaneously in a location ($3 \times 4\ \mu m^2$) where Fe and Br were clearly identified: (a) μ-PIXE spectra fitted with GUPIXWIN; (b) μ-EBS spectra fitted with DataFurnace. Coin: 5 Reais. Beam energy = 2.0 MeV.

Table 1
Elemental concentrations obtained from the GUPIXWIN fit to the μ-PIXE spectrum of Fig. 3a.

Element	Conc. [wt.%]
Fe	1.14 ± 0.01
Cu	6.58 ± 0.03
Br	0.78 ± 0.02
Ag	91.4 ± 0.7
Pb	0.110 ± 0.008

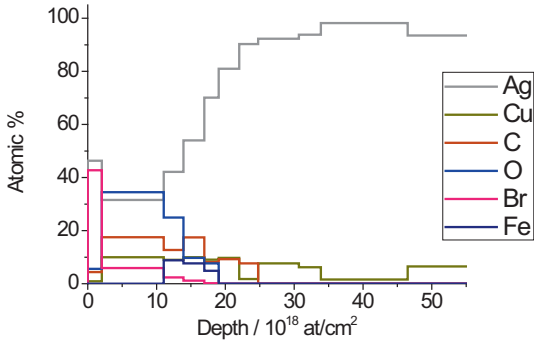

Fig. 4. Elemental depth profile obtained from the μ-EBS spectrum fit of Fig. 3b. Depth distribution for Pb is not plotted.

distribution maps (relative yield) for the K_α line of Ag (22.16 keV), the L_α line of Ag (2.98 keV) and the K_α lines of Cu (8.04 keV), Fe (6.40 keV) and Br (11.90 keV). A heterogeneous surface elemental distribution is clearly observed for these four elements. The two Ag maps also present some differences since the lower energy Ag L_α X-rays are more sensitive to surface inhomogeneities and to geometrical factors resulting from the coin embossment. μ-PIXE and μ-EBS spectra were taken simultaneously in the point ($3 \times 4\ \mu m^2$) marked with a dot in Fig. 1a, identified as having a clear X-ray Fe and Br signal. Fig. 3a) shows the μ-PIXE fitted spectrum, and Table 1 gives the elemental composition obtained from this fit using the Ag K lines for silver quantification. Due to the altered surface, a gradient concentration is expected and these results represent only average values over the proton range in the analyzed material.

The EBS spectrum shown in Fig. 3b) was fitted considering the information from the PIXE fit and included carbon and oxygen (not detectable by PIXE). Although the Ag amount evaluated from the PIXE spectrum relied in the Ag K line, total IBA fit of the EBS spectrum relies in the X-ray lines yield simulation considering both the Ag L and Ag K lines. This procedure ensures a better evaluation of the Ag depth profile, as it combines information from shallower layers (L lines) and deeper ones (K lines). Constraints to the layer model fit include: the simultaneous presence of Pb and Ag since they are usually associated in the metal ore; carbon, oxygen, iron and bromine presence is associated to the corroded superficial layer, so they were not allowed to be in the bulk; no elemental depth concentration constrains were imposed on Ag and Cu because the microstructure of Ag-Cu alloys can be inhomogeneous [16].

The self-consistent elemental depth profile thus obtained is shown in Fig. 4 (depth distribution not plotted for the very low concentration element Pb) and expressed numerically in Table 2. The depth scale is given in at/cm^2 (areal density), which can be converted into micrometer assuming an approximate density that results from a weighted density of each element detected. The DataFurnace code used a total 7 layers for describing the slowly varying concentration profiles in the corrosion layer plus 4 layers for the non-corroded bulk. It can be seen that the corrosion layer has a thickness of $\approx 20 \times 10^{18}$ at/cm^2 ($\approx 3.5\ \mu m$) where Fe and Br presence may result from dust particles incrusted at the surface of the metal, alongside with carbon and oxygen. It's essentially

Table 2
Elemental depth distribution (atomic %) obtained from the μ-EBS spectrum fit of Fig. 3b.

Layer	thickness [10^{15} at.cm^{-2}]	Ag	Cu	C	O	Br	Pb	Fe
1	2034	46.3	0.9	4.4	5.6	42.8	<0.1	0
2	9015	31.9	10.0	17.5	34.5	5.9	0.2	0
3	2869	42.2	9.0	12.7	24.9	2.4	<0.1	8.80
4	3031	54.0	10.0	17.4	9.8	1.2	<0.1	7.67
5	2085	70.1	9.1	8.2	7.6	0.2	<0.1	4.85
6	2972	81.0	9.8	9.2	0	0	<0.1	0
7	2762	90.3	1.8	7.7	0	0	0.2	0
8	5926	92.3	7.7	0	0	0	<0.1	0
9	3191	93.8	6.2	0	0	0	<0.1	0
10	12600	98.2	1.6	0	0	0	0.2	0
11	Bulk	93.5	6.5	0	0	0	<0.1	0

Please cite this article in press as: J. Cruz et al., Simultaneous use and self-consistent analyses of μ-PIXE and μ-EBS for the characterization of corrosion layers grown on ancient coins, Nucl. Instr. Meth. B (2017), http://dx.doi.org/10.1016/j.nimb.2017.02.010

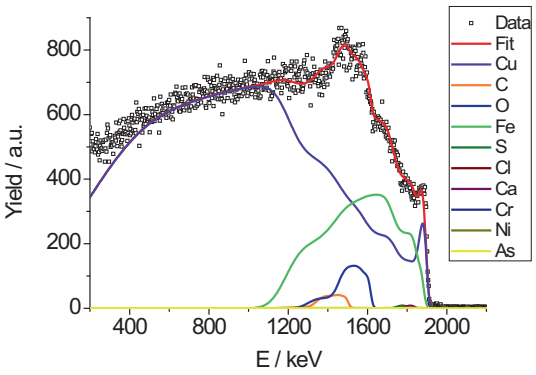

Fig. 5. μ-EBS spectrum taken in a location ($3 \times 4\ \mu m^2$) where Fe was clearly identified. Spectrum fitted with DataFurnace. Coin: 2 Reais. Beam energy = 2.0 MeV.

Table 3
Elemental concentrations obtained from the μ-PIXE spectrum fit.

Element	Conc. [wt.%]
S	1.14 ± 0.03
Cl	0.25 ± 0.02
Ca	0.339 ± 0.006
Cr	0.034 ± 0.002
Mn	0.248 ± 0.006
Fe	24.31 ± 0.08
Ni	0.14 ± 0.02
Cu	73.3 ± 0.2
As	0.11 ± 0.01

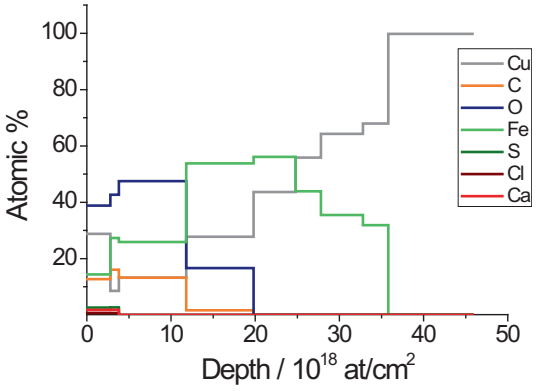

Fig. 6. Elemental depth profile obtained from the μ-EBS spectrum fit of Fig. 5. Depth distributions for As, Ni and Cr are not plotted.

the presence of these four elements that determines the depth distribution of silver at shallower layers. The obtained bulk composition is in close agreement with the original Ag alloy (91.66 Ag wt.%).

Due to the low concentration of lead (0.11 wt.%), the EBS spectra fit is largely insensitive to its presence. In these results there is a striking absence of Sulphur which should be copiously present in the corroded layer in the form of silver sulphide (Ag_2S), thus suggesting that the corrosion layer may have been artificially grown in order to make the coin look older or to mask some undue intervention at its surface.

3.2. Copper coin (2 Reais)

For the 2 Reais coin, a surface scan was taken in the area indicated by the open square in Fig. 1b. The detected X-rays indicated the presence of Cu (coin's major element) and also traces of Si, S, Cl, Ag, Ca, Ni, Cr, Fe, As and Pb with heterogeneous surface distributions.

Following the same procedure that was applied to the 5 Reais coin, μ-PIXE and μ-EBS spectra were taken simultaneously in a $3 \times 4\ \mu m^2$ point - dot marked in Fig. 1b – where Fe was clearly identified.

Fig. 5 shows the fitted μ-EBS spectrum. This fit was performed considering once again the data provided by PIXE (Table 3) and the ubiquitous presence of carbon and oxygen. Also, the coin's bulk composition was assumed to be almost pure copper, with the presence of the trace element As which is known to be intrinsically attached to the copper.

The self-consistent elemental depth profile thus obtained is shown in Fig. 6 (depth distributions not plotted for the very low concentration elements As, Ni and Cr) and Table 4. The DataFurnace code used a total 8 layers for describing the concentration profiles in the surface before reaching the coin bulk composition (fitted with 1 layer). It corresponds to an iron incrustation that extends as deep as $\approx 36 \times 10^{18}$ at/cm^2 (≈4.6 μm), showing a maximum concentration at a depth of $\approx 20 \times 10^{18}$ at/cm^2 (≈2.6 μm). This depth also defines the extension of the corroded layer, due to oxidation from the surface. Again, elements present in very small concentrations (Cr, Ni and As) have little influence on the EBS spectra fit which is largely insensitive to their presence.

4. Conclusions

Simultaneous and self-consistent μ-PIXE and μ-EBS analysis was applied to study the superficial corrosion layers of two XVI century Portuguese coins. The results revealed a complex multielemental depth concentration structure that would have been very hard to be obtained if we had not followed a self-consistent analysis using the "Total IBA" approach. The combination of PIXE and EBS at the experiment level and at the data analysis level has great advantages, since it showed that it is possible to characterize the superficial corroded layers in metals in terms of elemental composition and depth distribution in a non-destructive way. However, some care should be taken when considering the depth distribution of elements whose concentration is below 1–2%, since small variations on these contents usually do not contribute significantly

Table 4
Elemental depth distribution (atomic %) obtained from the μ-EBS spectrum fit of Fig. 5.

Layer	t [1e15 at.cm^{-2}]	Cu	C	O	Fe	S	Cl	Ca	Cr	Ni	As
1	2800	28.8	12.7	38.8	14.4	2.6	0.71	1.79	0.03	0.11	0.05
2	1000	8.5	16.1	42.7	27.3	2.6	0.69	1.82	0.03	0.11	0.06
3	8000	13.2	13.2	47.5	25.9	0	0	0	0.04	0.13	0.07
4	8000	27.7	1.66	16.6	53.8	0	0	0	0.03	0.10	0.05
5	5000	43.7	0	0	56.1	0	0	0	0.04	0.13	0.07
6	3000	55.8	0	0	43.9	0	0	0	0.04	0.15	0.07
7	5000	64.2	0	0	35.5	0	0	0	0.04	0.14	0.07
8	3000	67.9	0	0	31.8	0	0	0	0.04	0.12	0.06
9	Bulk	99.8	0	0	0	0	0	0	0	0.12	0.06

Please cite this article in press as: J. Cruz et al., Simultaneous use and self-consistent analyses of μ-PIXE and μ-EBS for the characterization of corrosion layers grown on ancient coins, Nucl. Instr. Meth. B (2017), http://dx.doi.org/10.1016/j.nimb.2017.02.010

to the variation of global EBS spectra. So, for these elements it is not possible to claim that the simulated depth distribution is the real one. However, it is a depth distribution that has restrictions imposed by the agreement between the simulated X-ray yields and PIXE yields.

The use of a micrometer sized proton beam for this study was also very important because it allowed probing regions with different degrees of corrosion.

Acknowledgements

J. Cruz acknowledges FCT-NOVA. V. Corregidor acknowledges FCT for the Ciência program and project UID/FIS/50010/2013 and L.C. Alves gratefully acknowledges the FCT support through the UID/Multi/04349/2013 project.

References

[1] C. Flament, P. Marchetti, Nucl. Instrum. Methods Phys. Res. B 226 (2004) 179–184, http://dx.doi.org/10.1016/j.nimb.2004.03.078.
[2] B.B. Tripathy, Tapash R. Rautray, A.C. Rautray, V. Vijayan, Appl. Radiat. Isot. 68 (3) (2010) 454–458, http://dx.doi.org/10.1016/j.apradiso.2009.12.031.
[3] H. Ben Abdelouaheda, F. Gharbi, M. Roumié, S. Baccouche, K. Ben Romdhane, B. Nsouli, A. Trabelsi, Mater. Charact. 61 (2010) 59–64, http://dx.doi.org/10.1016/j.matchar.2009.10.008.
[4] V. Corregidor, L.C. Alves, J. Cruz, Nucl. Instrum. Methods Phys. Res. B 306 (2013) 232–235, http://dx.doi.org/10.1016/j.nimb.2012.11.039.
[5] L. Beck, E. Alloin, C. Berthier, S. Réveillon, V. Costa, Nucl. Instrum. Methods Phys. Res. B 266 (2008) 2320–2324, http://dx.doi.org/10.1016/j.nimb.2008.03.084.
[6] M. Roumie, B. Nsouli, Y. Assafiri, Mater. Sci. Eng. 37 (2012) 012013, http://dx.doi.org/10.1088/1757-899X/37/1/012013.
[7] J. Cruz, V. Corregidor, L.C. Alves, Microsc. Microanal. 21 (Suppl. 6) (2015) 136–137, http://dx.doi.org/10.1017/S143192761401438X.
[8] C. Pascual-Izarra, N.P. Barradas, M.A. Reis, Nucl. Instrum. Methods Phys. Res. B 249 (2006) 820–822.
[9] N.P. Barradas, Surf. Interface Anal. 35 (2003) 760–769, http://dx.doi.org/10.1002/sia.1599.
[10] C. Jeynes, M.J. Bailey, N.J. Bright, M.E. Christopher, G.W. Grime, B.N. Jones, V.V. Palitsin, R.P. Webb, Nucl. Instrum. Methods Phys. Res. B 271 (2012) 107–118, http://dx.doi.org/10.1016/j.nimb.2011.09.020.
[11] L.C. Alves, M.B.H. Breese, E. Alves, A. Paúl, M.R. da Silva, M.F. da Silva, J.C. Soares, Nucl. Instrum. Methods Phys. Res. B 161–163 (2000) 334–338, http://dx.doi.org/10.1016/S0168-583X(99)00768-5.
[12] G.W. Grime, M. Dawson, Nucl. Instrum. Methods Phys. Res. B 104 (1995) 107–113, http://dx.doi.org/10.1016/0168-583X(95)00401-7 (95)00401-7.
[13] J.A. Maxwell, W.J. Teesdale, J.L. Campbell, Nucl. Instrum. Methods Phys. Res. B 95 (1995) 407, http://dx.doi.org/10.1016/j.nimb.2004.06.044.
[14] S.L. Molodtsov, A.F. Gurbich, Nucl. Instrum. Methods Phys. Res. B 267 (2009) 3484–3487.
[15] A. Gurbich, SigmaCalc 1.6 <http://www-nds.iaea.org/sigmacalc/>.
[16] L. Beck, S. Besonnet, S. Réveillon, D. Eliot, F. Pilon, Nucl. Instrum Methods Phys. Res. B 226 (2004) 153–162, http://dx.doi.org/10.1016/j.nimb.2004.06.044.

Please cite this article in press as: J. Cruz et al., Simultaneous use and self-consistent analyses of μ-PIXE and μ-EBS for the characterization of corrosion layers grown on ancient coins, Nucl. Instr. Meth. B (2017), http://dx.doi.org/10.1016/j.nimb.2017.02.010